Free Radical Research, May 2008; 42(5): 442–455

informa
healthcare

LC/ESR/MS study of spin trapped carbon-centred radicals formed from *in vitro* lipoxygenase-catalysed peroxidation of γ-linolenic acid

QINGFENG YU[1,2], ZHEN SHAN[1], KUNYI NI[2], & STEVEN Y. QIAN[1]

[1]*Department of Pharmaceutical Sciences, College of Pharmacy, Nursing, and Allied Sciences, North Dakota State University, Fargo, ND, 58105, USA, and* [2]*Department of Analytical Chemistry, China Pharmaceutical University, Nanjing, 210009, China*

Accepted by Professor M. Davies

(Received 5 December 2007; in revised form 22 February 2008)

Abstract

γ-Linolenic acid (GLA) has been reported as a potential anti-cancer and anti-inflammatory agent and has received substantial attention in cancer care research. One of the many proposed mechanisms for GLA biological activity is free radical-mediated lipid peroxidation. However, no direct evidence has been obtained for the formation of GLA-derived radicals. In this study, a combination of LC/ESR and LC/MS was used with α-[4-pyridyl-1-oxide]-N-*tert*-butyl nitrone (POBN) to profile the carbon-centred radicals that are generated in lipoxygenase-catalysed GLA peroxidation. A total of four classes of GLA-derived radicals were characterized including GLA-alkyl, epoxyallylic, dihydroxyallylic radicals and a variety of carbon-centred radicals stemming from the β-scissions of GLA-alkoxyl radicals. By means of an internal standard in LC/MS, one also quantified each radical adduct in all its redox forms, including an ESR-active form and two ESR-silent forms. The results provided a good starting point for ongoing research in defining the possible biological effects of radicals generated from GLA peroxidation.

Keywords: *Electron spin resonance, free radicals, HPLC, lipid peroxidation, mass spectrometry, spin trapping*

Abbreviations: *ACN, acetonitrile; EIC, extracted ion current; ESR, electron spin resonance; GLA, gamma linolenic acid (all-*cis*-6, 9, 12-octadecatrienoic acid); HOAc, glacial acetic acid; HPLC (LC), high performance liquid chromatography; I.S., internal standard; LA, linoleic acid (*cis, cis*-9, 12-octadecadienoic acid); LOX, lipoxygenase; L•, lipid alkyl radicals; •L(OH)$_2$, lipid dihydroxyallylic radicals; MRM, multiple reaction monitoring; OL•, lipid epoxyallylic radicals; POBN, α-[4-pyridyl-1-oxide]-N-*tert*-butyl nitrone; PUFAs, polyunsaturated fatty acids; TIC, total ion current; t_R, retention time.*

Introduction

The fatty acid γ-linolenic acid (all-*cis*-6, 9, 12-octadecatrienoic acid, GLA) is a member of a group of ω-6 polyunsaturated fatty acids (PUFAs) that are mostly present in vegetable oils, such as evening primrose oil, blackcurrant seed oil, borage oil and hemp seed oil. The human body can obtain GLA either by biosynthesis from linoleic acid (all-*cis*-9, 12-octadecadienoic acid, LA) or through dietary supplements. Unlike many other ω-6 PUFAs, which tend to be unhealthy, GLA is important to maintaining good human health in a variety of ways [1]. As a dietary supplement, GLA can improve the clinical symptoms of many diseases, such as autoimmune disorders, arthritis and eczema [2–5].

Correspondence: Steven Y. Qian, PhD, Department of Pharmaceutical Sciences, College of Pharmacy, Nursing, and Allied Sciences, North Dakota State University, Fargo, ND 58105, USA. Tel: (701) 231-8511. Fax: (701) 231-8333. Email: steven.qian@ndsu.edu

ISSN 1071-5762 print/ISSN 1029-2470 online
DOI: 10.1080/10715760802085344

Considerable research activity is being focused on the mechanism of cytotoxity of GLA in cancer cells. At certain concentrations, GLA exhibits anti-tumour activity by inhibiting the growth and metastasis of a variety of tumour cells, including prostate [6], breast [7,8], superficial bladder [9,10] and pancreatic [11] cancer, as well as human gliomas [12,13]. GLA attenuates prostate carcinogenesis *via* the generation of 15-hydroxyeicosatrienoic acid [14] and also reduces cancer cell adhesion and cell motility by decreasing secretion of osteonectin [15]. Interestingly, GLA executes its anti-cancer activity with little or no effect on survival of normal cells [16]. Among the many proposed mechanisms to which GLA biological activity is attributed, the most popular is free radical-mediated lipid peroxidation [17–20]. However, primarily due to the lack of appropriate methodologies, no direct evidence has previously been found for formation of free radicals in its peroxidation.

Lipid peroxidation is a well-known free radical chain reaction in which many types of free radicals are formed in three steps: initiation, propagation and termination [21,22]. The starting point for study of GLA's potential bioactivity is to determine what kinds and amounts of free radicals could be formed in its peroxidation. Such unstable free radicals can be studied with the unique method of electron spin resonance (ESR) spin trapping [23–27]. In this technique, spin trap compounds are used to convert unstable free radicals to relatively stable radicals (spin adducts) in order to measure them by ESR. One of these trapping agents, the nitrone compound α-[4-pyridyl-1-oxide]-N-*tert*-butyl nitrone (POBN), preferentially reacts with unstable carbon-centred free radicals and has been used successfully to study lipid-derived radicals formed from peroxidation of many PUFAs *in vitro* and *in vivo* [25–28].

However, since many POBN adducts share identical or similar hyperfine couplings [29], the six-line ESR spectra that are typically observed for POBN adducts in such studies cannot give us complete structural and quantitative information for individual trapped radicals. To overcome this ESR limitation, the LC/ESR and LC/MS techniques have recently been developed [30–32], enabling us to successfully identify free radicals trapped with POBN formed from lipid peroxidation of a number of PUFAs.

In the present work, we have used a combination of LC/ESR and LC/MS to profile spin adducts of carbon-centred radicals formed from soybean lipoxygenase (LOX)-catalysed GLA peroxidation in the presence of POBN. A total of four classes of radicals were trapped and identified, including lipid alkyl radicals ($L^{\bullet}$), lipid epoxyallylic radicals ($OL^{\bullet}$), lipid dihydroxyallylic radicals ($^{\bullet}L(OH)_2$) and a variety of radicals formed from β-scission of lipid alkoxyl radicals. Using an appropriate internal standard, we have also comprehensively quantified each POBN adduct by simultaneously profiling all three of its redox forms: the ESR-active POBN adduct itself and the ESR-silent hydroxylamine and nitrone adducts. Our results show a great improvement in the sensitivity and reliability of radical detection and provide a good starting point for our ongoing research on the bioactivity associated with GLA-derived radicals.

Materials and methods

Reagents

Ethyl alcohol, glacial acetic acid (HOAc), soybean lipoxygenase (LOX, Type I-B) and ascorbic acid were purchased from Sigma Chemical Co. (St. Louis, MO). γ-Linolenic acid (GLA) was purchased from Nu-Chek-Prep Inc. (Elysian, MN). High purity α-[4-pyridyl-1-oxide]-N-*tert*-butyl nitrone (POBN) was purchased from Alexis Biochemicals (San Diego, CA). Deuterium α-[4-pyridyl-1-oxide]-N-*tert*-butyl nitrone (D_9-POBN) was obtained from CDN Isotopes Inc. (Pointe-Claire, QC, Canada). Chelex 100 (200–400 mesh sodium form) was obtained from Bio-Rad Laboratories Inc. (Hercules, CA). Acetonitrile (ACN, HPLC grade) and water (H_2O, LC-MS grade) were purchased from Mallinckrodt Baker Inc. (Phillipsburg, NJ) and EMD Chemicals Inc. (Gibbstown, NJ), respectively.

Reaction conditions

GLA peroxidation experiments were performed in 50 mM (pH 7.5) phosphate buffer solution. Metal ions in phosphate buffer solution were chelated with Chelex 100 resin and solution was confirmed as virtually metal-free by passing the ascorbic acid assay [33]. The complete reaction mixture containing 1 mM GLA (in 1% ethyl alcohol), 20 mM POBN and 20 Kunits/ml soybean lipoxygenase was continuously stirred at 37°C and 400 rpm on a Thermo-Shaker (Boekel Scientific, Feasterville, PA) in the absence of light.

We found that mixing reaction samples with $>20\%$ ACN (v/v) could improve the reliability of real time formation of POBN radical adducts since it completely denatured the LOX enzyme and immediately stopped enzyme-mediated peroxidation. Thus, at each experimental time point (0.5, 1, 2, 5, 15, 30, 45 and 60 min), aliquots were taken and mixed immediately with an equal volume of ACN. After the LOX enzyme was precipitated and separated from the ACN-sample mixtures with a Microfuge^{R} 22R Centrifuge (Beckman Coulter Inc, Fullerton, CA) at 5000 rpm 15 min, the sample solutions were ready for off-line ESR analysis for real time radical formation. For on-line LC/ESR and LC/MS analysis, however, the above enzyme-free ACN-sample mixtures were further transferred into

new tubes and placed in a Vacufuge™ 5301 Concentrator (Eppendorf, Hamburg, Germany), where most of the ACN was evaporated at room temperature in ~15 min. Either LC/ESR/MS analysis was then carried out immediately on these enzyme-free condensed sample solutions, or they were stored at −80°C for later analysis.

ESR measurements

Off-line ESR. For the complete reaction system and control experiments, reaction solutions (with or without mixing with ACN) were transferred to the same ESR flat cell for magnetic field scans. ESR spectra were obtained with a Bruker EMX spectrometer equipped with a super high Q cavity operating at 9.78 GHz and room temperature. Other ESR spectrometer settings were: magnetic field centre, 3494.4 G; magnetic field scan, 70 G; modulation frequency, 100 kHz; microwave power, 20 mW; modulation amplitude, 1.0 G; receiver gain, 5.0×10^4; time constant, 0.655 s; and conversion time, 0.164 s.

On-line LC/ESR. The on-line LC/ESR system consisted of an Agilent 1200 series HPLC system and the above Bruker EMX ESR system. The outlet of the Agilent UV detector was connected to a highly sensitive Aquax ESR cell with red peek HPLC tubing (0.005 in i.d.). The POBN radical adducts were monitored *via* UV absorption in the HPLC at 265 nm [34,35] followed by ESR. There was a 9 s delay between the UV (HPLC system) and ESR detection.

LC separations were performed on a C_{18} column (ZORBAX Eclipse-XDB, 3.0×75 mm, 3.5 μm) equilibrated with solvent A (H_2O-0.1% HOAc). The enzyme-free condensed sample solution (40 μl) was typically injected into the HPLC column by autosampler and eluted at 0.8 ml/min flow rate with gradient elutions of (i) 0–40 min: 100% to 30% of solvent A, 0% to 70% of solvent B (ACN-0.1% HOAc); (ii) 40–45 min 30% to 5% of A, 70% to 95% of B; (iii) 45–54 min 5% of A and 95% of B and (iv) 54–60 min 5% to 100% of A and 95% to 0% of B.

On-line ESR monitoring consisted of a time scan with the magnetic field fixed on the maximum of the first line of off-line ESR spectra. Other ESR spectrometer settings were: modulation frequency, 100 kHz; modulation amplitude, 3.0 G; microwave power, 20 mW; receiver gain, 4×10^5; and time constant, 2.6 s.

LC/MS measurements

The LC/MS system consisted of an Agilent 1200 LC system and an Agilent LC/MSD Trap SL Mass Spectrometer. The outlet of the UV detector was connected to the MS system with Red peek HPLC tubing (0.005 in. i.d.) as well. Chromatographic conditions were identical to those used for on-line LC/ESR. However, the LC flow rate (0.8 ml/min) was adjusted so as to direct 30 ~ 40 μl/min into the MS inlet via a splitter. There was ~35 s delay between the UV detection and the MS detection. Positive ions from electrospray ionization (ESI) were analysed for all LC/MS and LC/MS^2 experiments.

TIC and EIC (LC/MS). Total ion current (TIC) chromatogram in full mass scan mode (m/z 150 to m/z 600) was performed to profile all products formed from LOX-catalysed GLA peroxidation *in vitro* in the presence of POBN. Other MS settings were: capillary voltage, −4500 V; nebulizer press, 20 psi; dry gas follow rate, 8 L/min; dry temperature, 60°C; compound stability, 20%; and number of scans, 50. An extracted ion current (EIC) chromatogram from the above full scan experiment was obtained to acquire the MS profile matching the POBN trapped radical adducts that were monitored as ESR-active peaks in on-line LC/ESR. An isolation width of m/z ± 0.5 Da was used in EICs of molecule ions of interest.

LC/MS^2 identification. LC/MS^2 analysis in multiple reaction monitoring (MRM) mode was performed to confirm the structural assignment of each ESR-active POBN adduct as well as its two ESR-silent forms. A 4-Da width was typically used to isolate parent ions of interest, including all redox forms of each POBN adduct. Other settings were: mass range, m/z 100–m/z 600; capillary voltage, −4500 V; nebulizer press, 20 psi; dry gas follow rate, 8 L/min; dry temperature, 60°C; compound stability, 20%; and number of scans, 5.

The LC/MS^2 studies of D_9-POBN spin trapped products were performed for any peaks of POBN adducts or/and related redox forms whose structures would not be clearly reflected by fragmentation pattern of LC/MS^2 spectra with POBN alone [36,37]. All reaction conditions of the D_9-POBN spin trap experiments were the same as the corresponding POBN spin trapping reaction system with POBN replaced by the same amount of D_9-POBN.

LC/MS quantification. In LC/MS quantification, a small and known amount of D_9-POBN was used purely as an internal standard, unlike the above LC/MS^2 procedure in which D_9-POBN was used as a spin trap for the purpose of structure identification. For quantification, D_9-POBN was not added until after the analyte was mixed with a stop-solution (ACN) to completely denature the LOX enzymes, at which point it could not act as a spin trap. Based on the average abundance of many types of POBN radical adducts observed in our complete reaction system within 1 h of reaction, we chose 3.8 μg/ml as the quantity of internal standard D_9-POBN to add to the ACN-sample mixture. To quantify the abundance of molecule ions of interest, the integrated EIC at m/z

204 for 3.8 μg/ml D_9-POBN was always used as a standard. The injection volume of LC/MS for quantification was adjusted to 20 μl. Other LC/MS settings were identical to those of the full scan methods in the previous section.

Results

Off-line ESR study of POBN adducts generated from LOX-catalysed GLA peroxidation

For the complete GLA peroxidation system containing GLA, LOX and POBN, ESR spectroscopy gave a six line ESR signal with hyperfine coupling constants of $a^N \approx 15.69$ G and $a^H \approx 2.68$ G (Figure 1A) that is typical of POBN spin-trapped adducts. In the absence of POBN, no ESR signal was observed (Figure 1B), indicating that all GLA-derived radicals thus formed are too short-lived to be detected by ESR and that spin traps such as POBN are needed for trapping and observing these unstable radicals by ESR. In the control experiment in the absence of LOX (Figure 1C), a very weak signal was observed because trace metal ions can initiate a limited amount of GLA autoxidation. In the control experiment excluding GLA (Figure 1D), $\sim 1/10$ of the ESR signal intensity of that of the complete reaction system (Figure 1A) was observed. Since the hyperfine couplings ($a^N \approx 15.71$ G and $a^H \approx 2.62$ G, Figure 1D) were consistent with previous studies [30,31], this signal was assigned as the POBN adduct of hydroxyethyl radical formed from ethanol oxidation (adding GLA stock solution was replaced by adding the equal volume of ethanol). The significantly increased intensity of the ESR in Figure 1A compared to Figures 1B–D suggests that the radicals formed in the complete reaction system mainly resulted from LOX-catalysed GLA peroxidation.

As shown in Figure 1, the POBN spin trap technique facilitated ESR detection of carbon-centred radicals from GLA peroxidation. However, lipid peroxidation is a very complicated reaction in which many types of radicals could form and be trapped in the presence of spin traps. It is impossible to distinguish either numbers or types of carbon-centred radicals from such ESR spectra as Figure 1A because many POBN radical adducts share the same or similar hyperfine couplings [29]. To overcome this shortcoming of ESR, we used a combination of LC/ESR and LC/MS [30–32,36,37].

In order to subject our sample solution to a high throughput LC/ESR and LC/MS analysis, we tested the effects of the organic solvent acetonitrile (ACN) on denaturation of LOX enzyme and attenuation of the off-line ESR signal intensity. Mixing samples with different volumes of ACN (5–70%, v/v) do not interfere with determining the structures of the POBN adducts formed, except for the dilution effect on ESR similar to that of diluting with H_2O or/and buffer solution (data not shown). When ACN at proportion $> 20\%$ (v/v) was mixed with the complete reaction system before the enzyme was added, no ESR signal was detected since LOX activity was

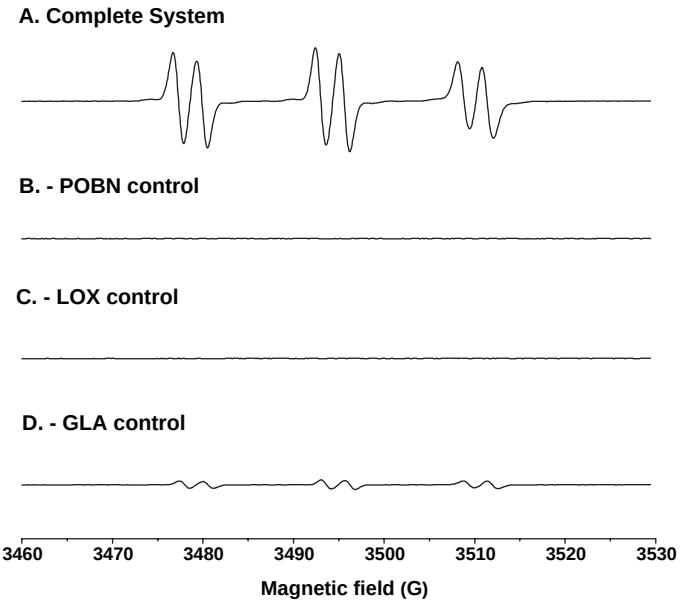

Figure 1. Off-line ESR spectra from the complete GLA-peroxidation system and the relevant control experiments. (A) ESR spectrum of the complete system at 30 min reaction time. The complete system (50 mM phosphate buffer, pH 7.5) contained 20 mM POBN, 1 mM GLA (in 1% ethanol) and 2×10^4 Units/ml LOX. An ESR field scan (70 G) was performed and the hyperfine couplings of this spectrum were $a^N \approx 15.69$ G and $a^H \approx 2.68$ G; (B and C) ESR spectra of POBN and LOX control experiments. ESR field scans were performed at 30 min reaction time for the complete reaction mixtures absent POBN and LOX, respectively; (D) ESR spectrum of control experiment of GLA. Reaction mixture excluding GLA (adding GLA stock solution was replaced by adding the same volume of ethanol) was subjected to ESR field scan at 30 min. Hyperfine coupling constants of this spectrum were $a^N \approx 15.71$ G, $a^H \approx 2.62$ G.

completely inhibited. Therefore, at each experimental time point, the reaction was stopped by adding an equal volume of ACN to make a 50% (v/v) sample mixture for high throughput analysis.

LC/ESR/MS and LC/MS^2 study of ESR-active products: Identification of POBN adducts

When a gradient separation is performed in conjunction with a large injection of sample containing an organic solvent, many analytes could be eluted out immediately. Even a small portion of organic solvent, *e.g.* $>5\%$ ACN in our case, in the sample mixture could elute sufficient analyte in the mobile phase to create very poor retention behaviour in the LC separation. Therefore, in order to have a reliable chromatographic separation of analyte, the above ACN-sample solution mixtures (50% v/v) were subjected to evaporation of all the added ACN (returning to the previous volume) before on-line LC/ESR and LC/MS analysis.

A UV chromatogram (absorption at 265 nm) of the above enzyme-free condensed sample was then obtained, as shown in Figure 2A. Among many eluents, only a few were ESR active; some of these could be matched with the corresponding UV absorptions (marked with t_Rs and peak numbers, Figures 2A and B). Under the same chromatographic conditions, the ESR active peaks (peaks 2–7, Figure 2B) were also profiled for their possible molecule ions (m/z 240, m/z 296, m/z 336s and m/z 266) in a full scan or total ion chromatogram (TIC) of LC/MS (Figure 2C), respectively. An extracted ion chromatogram (EIC, Figure 2D) gave an MS profile closely similar to the one from on-line ESR (Figure 2B) when these four molecule ions were selected. Assignments of all ESR-active peaks in Figure 2B were made following LC/MS^2 analysis with regard to the proposed mechanism (Scheme 1).

The ESR-active peak 2 and its related EIC peak ($t_R \approx 9.2$ min, m/z 240, Figures 2B and D) most likely corresponded to the POBN adduct of hydroxyethyl radical ($^\bullet C_2H_4OH$) [30–32] which was formed via ethanol oxidation (ethanol was used to prepare the GLA stock solution). The LC/MS^2 spectrum of the m/z 240 ion (Figure 3A) in the ESR-active peak 2 was consistent with the fragmentation pattern of POBN/$^\bullet C_2H_4OH$ published elsewhere [30–32] and thus confirmed the assignment of this structure.

The ESR-active peak 3 and its related EIC peak ($t_R \approx 11.8$ min, m/z 296, Figures 2B and D) appeared to correspond to the POBN adduct of the radical generated from β-scission of the 6-GLA-alkoxyl radical, POBN/$^\bullet C_5H_9O_2$ (Scheme 1). This assignment was confirmed by its LC/MS^2 (Figure 3B), which showed the main fragmentation ions of POBN/$^\bullet C_5H_9O_2$.

The ESR-active peaks 4–6 and their EIC peaks ($t_R \approx 15.6$, 17.3 and 17.7 min, m/z 336, Figures 2B and D) most likely corresponded to three isomers of the POBN adduct of $^\bullet C_8H_{13}O_2$. Such radicals are generated from β-scission of the 9-GLA-alkoxyl radical (Scheme 1). The main fragmentation ions shown in the LC/MS^2 of the m/z 336 ion in the ESR-active peak 4 (Figure 3C) confirmed the structure assignment to POBN/$^\bullet C_8H_{13}O_2$. However, there was not enough evidence from the fragmentation ions in LC/MS^2 of peaks 4–6 to distinguish the difference among those isomers (data not shown).

The ESR-active peak 7 and its EIC peak ($t_R \approx 21.2$ min, m/z 266, Figures 2B and D) appeared to be the POBN adduct of pentyl radical ($^\bullet C_5H_{11}$) generated from β-scission of the 13-GLA-alkoxyl radical because the protonated molecule ion of m/z 266 was observed, consistent with the proposed GLA peroxidation mechanism (Scheme 1). This assignment was confirmed when the main fragmentation ions of POBN/$^\bullet C_5H_{11}$ appeared in the LC/MS^2 of the m/z 266 ion in peak 7 (Figure 3D). The fragmentation pattern of Figure 3D was also consistent with our previous studies [31].

There were other ESR-active products, such as peak 1 in Figure 2B (where more than one isomer might exist based on the poor peak shape) that were much more difficult to match with their protonated molecule ions, since no matching sets of peaks were found among on-line UV, on-line ESR and on-line MS (Figures 2A–C). This phenomenon often occurs when adducts of very low abundance are co-eluted with other major components. For example, the chance to profile or extract possible molecules around the ESR-active peak 1 ($t_R \approx 7.3$–7.5 min) was completely lost when the dominant m/z 195 ion was co-eluted due to the necessary overdose of POBN spin trap.

Indeed, to distinguish a limited amount of different radical adducts from the large POBN peak (m/z 195) represents a challenge in LC/MS. According to our previous observations, all peaks that co-eluted with POBN very likely corresponded to the isomers of POBN adducts of polar radicals, such as the dihydroxylinolenic acid radical $^\bullet L(OH)_2$, that were formed during LOX-catalysed peroxidation of many PUFAs [30–32]. To test for this possibility in GLA peroxidation (Scheme 1), a D_9-POBN spin trapping experiment was also conducted for the same LOX-catalysed peroxidation. Here solid evidence for the above assignments was provided by the similarity of fragmentation patterns in the LC/MS^2 of the m/z 506 ion (Figure 3E) at $t_R \approx 7.3$–7.5 min (the POBN adduct of $^\bullet L_{GLA}(OH)_2$) to those of the LC/MS^2 (Figure 3F) for the m/z 515 ion (the D_9-POBN adduct of $^\bullet L_{GLA}(OH)_2$).

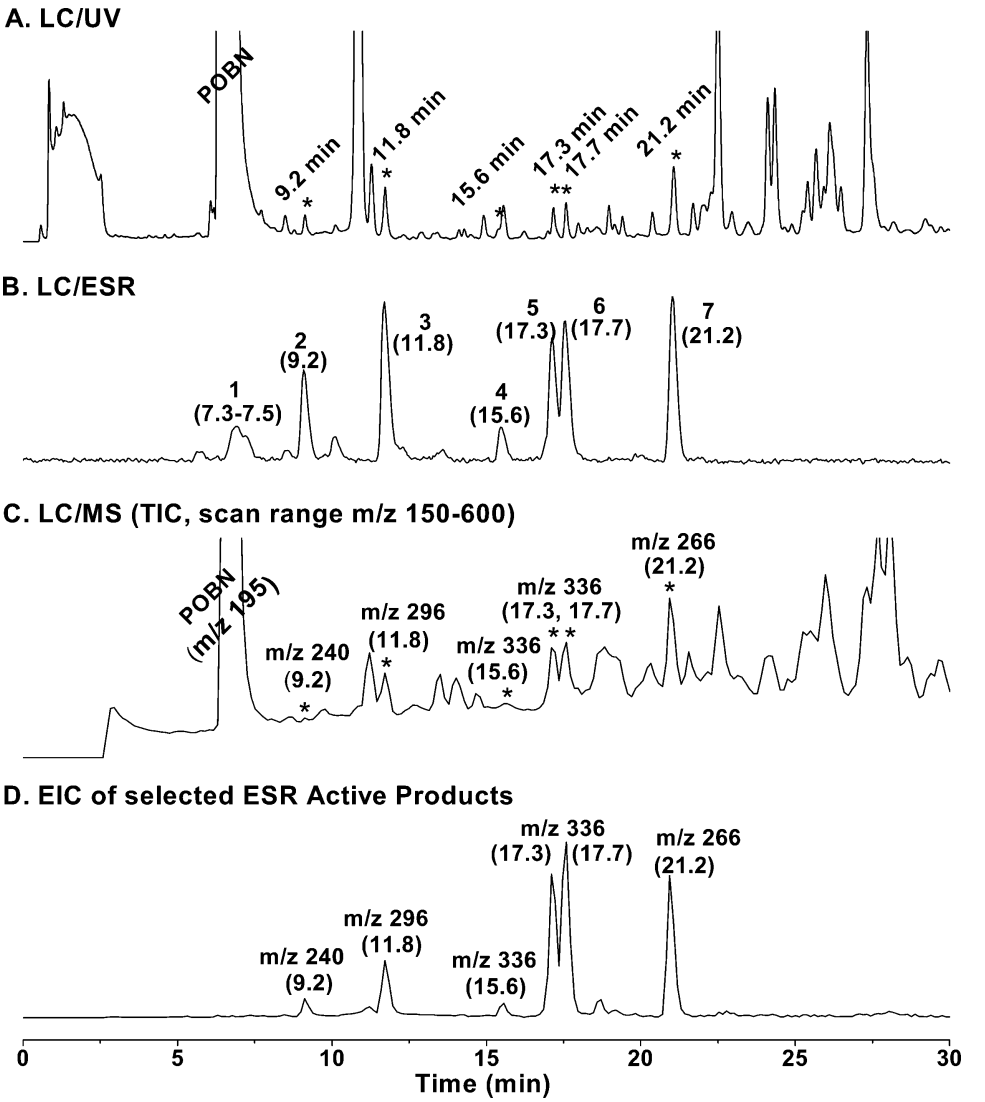

Figure 2. On-line LC/ESR and LC/MS chromatogram of the enzyme-free, condensed ACN-sample mixture from the experiment in Figure 1A. (A) UV chromatographic separation was performed at an absorption of 265 nm with a C_{18} column (ZORBAX Eclipse-XDB, 3.0 × 75 mm, 3.5 μm) equilibrated with solvent A (H_2O-0.1% HOAc). Conditions of gradient elution were described in Methods; (B) ESR chromatogram was obtained in an ESR spectrometer equipped with an Aquax ESR cell. A time scan was performed with the magnetic field fixed on the maximum of the first line of Figure 1A. There was a 9 s offset due to the connections between the UV detector and the ESR. On-line ESR settings were described in Methods; (C) On-line MS (full scan or total ion chromatogram, TIC, m/z 150 to m/z 600) was obtained with chromatographic conditions identical to those in on-line ESR. The LC flow rate (0.8 ml/min) was adjusted to 30 ~ 40 μl/min into the MS inlet with a splitter; the first three min of LC eluants were always by-passed and not analysed for their MS. Between UV and MS measurements there was a 35 s offset due to the connection settings. On-line MS settings were described in Methods; (D) Extracted ion current (EIC) chromatogram of four ions of (m/z 240, m/z 336, m/z 266 and m/z 296) from the above full scan was obtained for the MS profile matching the POBN adducts that were monitored as ESR-active peaks in on-line ESR.

LC/MS study of ESR-silent products: Identification of redox forms of POBN adducts

Free radicals, including radical adducts, can be either reduced or oxidized during a system's reaction, depending on the individual redox environment. Under our reaction conditions, the ESR-active forms of POBN radical adducts could be converted to either of two ESR-silent redox forms of the POBN adducts, namely, nitrone adduct and hydroxylamine (Scheme 1). Thus, measuring free radical adducts in their ESR-silent forms in addition to observing the ESR-active form represents a great improvement in the method's sensitivity and reliability. The reduction and/or oxidation of any given POBN adduct corresponded to the structural changes within ± 1 Da for the protonated molecules during MS ionization (Scheme 1).

When the m/z 267 ion and m/z 265 ions were extracted from the TIC (Figure 2C) to profile the ESR-silent forms of the POBN adduct of $^{\bullet}C_5H_{11}$ (m/z 266, ESR-active peak 7), an EIC peak of m/z 267, potentially the reduced product, was separated at $t_R \approx 15.1$ min (Figure 4A), while two EIC peaks of m/z 265, with $t_R \approx 11.5$ and 19.1 min, appeared to be two isomers of potentially oxidized

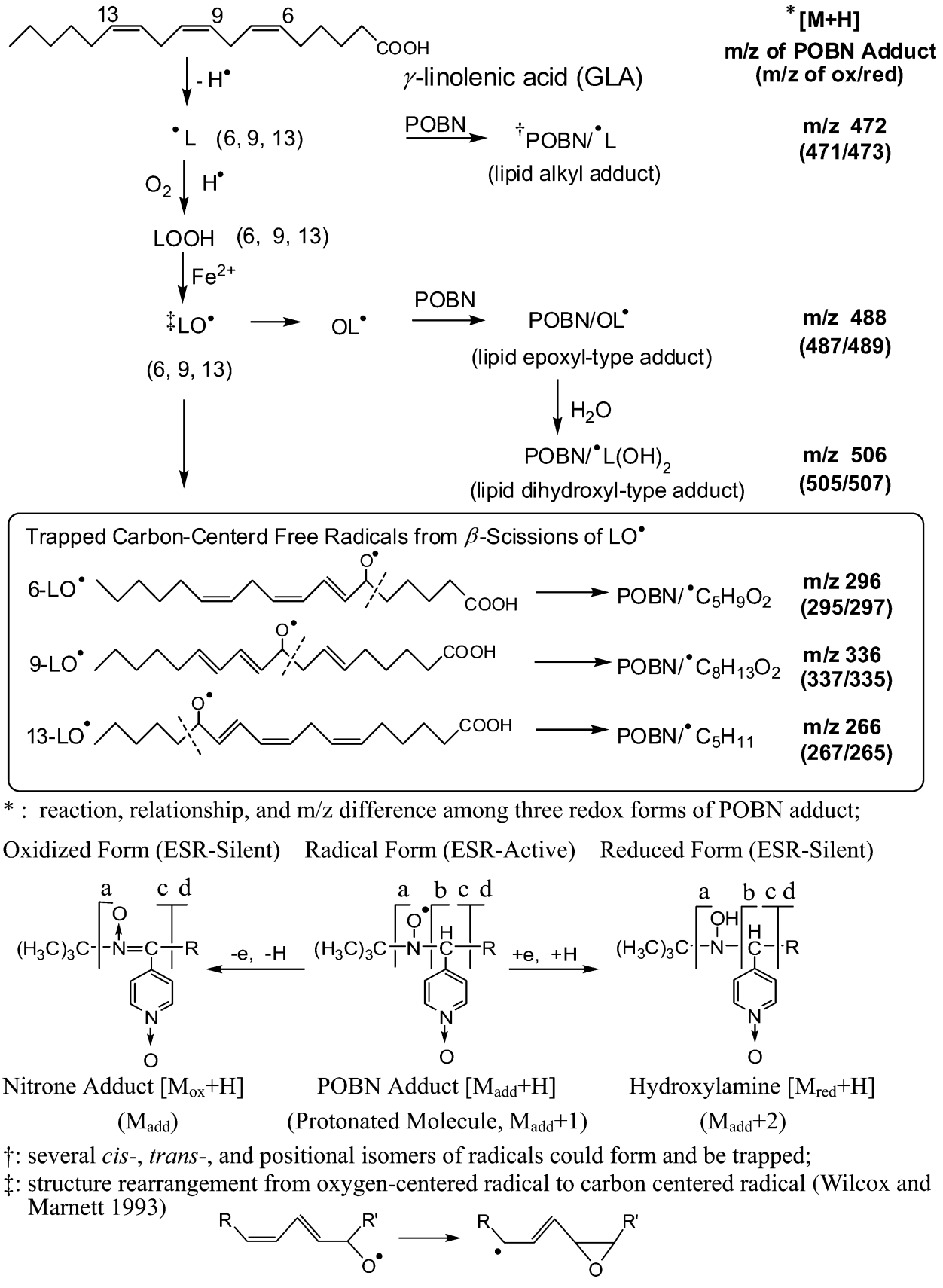

* : reaction, relationship, and m/z difference among three redox forms of POBN adduct;

†: several *cis*-, *trans*-, and positional isomers of radicals could form and be trapped;

‡: structure rearrangement from oxygen-centered radical to carbon centered radical (Wilcox and Marnett 1993)

Scheme 1. Chemistry of formation of spin adducts of GLA-derived carbon-centred radicals in LOX-catalysed GLA peroxidation, the subsequent redox reaction and relationship of the three redox forms of the POBN adduct.

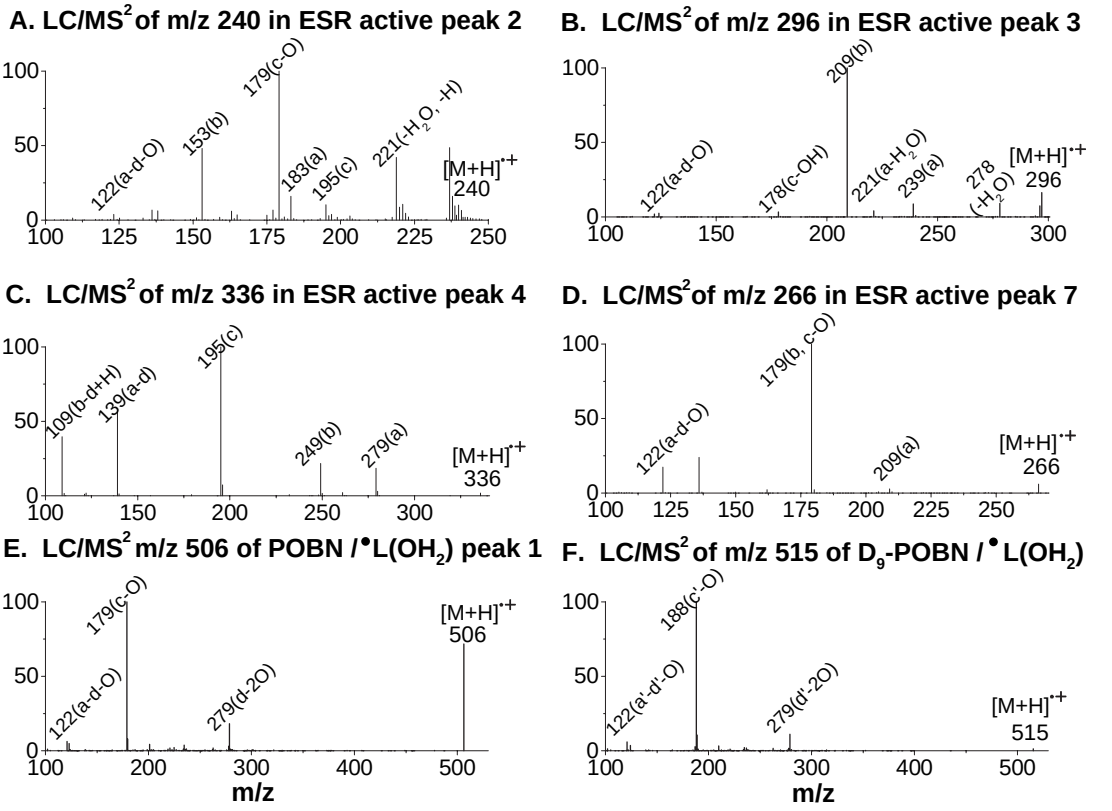

Figure 3. LC/MS^2 spectra of selected POBN adducts that were ESR-active peaks in Figure 2B. (A) LC/MS^2 of m/z 240 ion for ESR-active peak 2; (B) LC/MS^2 of m/z 296 ion for ESR-active peak 3; (C) LC/MS^2 of m/z 336 ion for ESR-active peak 4 (similar LC/MS^2 spectra were also observed for ESR-active peaks 5 and 6); (D) LC/MS^2 of m/z 266 ion for ESR-active peak 7; (E) LC/MS^2 of m/z 506 ion for ESR-active peak 1; and (F) LC/MS^2 of m/z 515 ion from D_9-POBN experiment relevant to ESR-active peak 1 in E. Note that the fragmentation patterns and '*a*', '*b*', '*c*' and '*d*' ions of all tested POBN adducts were consistent with the LC/MS^2 of POBN adducts published elsewhere [30,31] as well as the pattern described in Scheme 1. D_9-POBN-related products always have retention times ~12 s shorter than its POBN counterpart under our chromatography conditions. Some unique characters were observed between each counterpart of POBN vs D_9-POBN experiment due to fragmentations with/without the loss of the *tert*-butyl group ('*a*' and '*b*' ions/'*c*' ion).

products (Figure 4B). LC/MS^2 analysis of the POBN spin adducts confirmed these assignments with fragmentation patterns of the m/z 267 and m/z 265 ions, respectively (insets of Figures 4A and B). However, the LC/MS^2 for the m/z 265 ions at $t_R \approx 11.5$ and 19.1 min did not provide enough information to differentiate between the isomers.

Similarly, ions of m/z 297 and m/z 295 were extracted (Figures 4C and D) as possible ESR-silent forms of POBN/$^\bullet C_5H_9O_2$. The reduced product (m/z 297 ion) of this adduct was separated at $t_R \approx 8.1$ min, while two oxidized products (m/z 295) were profiled at $t_R \approx 6.8$ and 11.7 min. The subsequent LC/MS^2 studies confirmed these assignments as shown in the insets of Figures 4C and D, respectively. Again, there was not enough evidence from the LC/MS^2 for the m/z 295 ions at $t_R \approx$ 6.8 and 11.7 min to distinguish between the isomers.

We observed many isomers of the ESR-active product POBN/$^\bullet C_8H_{13}O_2$ in GLA-catalysed peroxidation; about six possible isomers of their reduced products (m/z 337) were extracted at $t_R \approx 14.6$, 36.4, 39.4, 40.7, 41.5 and 42.5 min (Figure 4E). The main fragmentation patterns in the LC/MS^2 spectra of the m/z 337 ions further confirmed this structural assignment (inset of Figure 4E). At least six potentially oxidized products of POBN/$^\bullet C_8H_{13}O_2$ were profiled at $t_R \approx 10.6$, 11.4, 16.5, 17.7, 18.7 and 20.0 min as m/z 335 ions (Figure 4F) and the main fragmentation patterns in their LC/MS^2 confirmed the structural assignment (inset of Figure 4F). However, the fragmentation ions in the LC/MS^2 presented no solid evidence from different fractions of the m/z 335 or m/z 337 ions that could be used to differentiate among isomers.

Unlike other POBN adducts whose reduced products were always detected, we only separated possible oxidized product(s) of POBN/$^\bullet L_{18:3}(OH)_2$ as the m/z 505 ion at $t_R \approx 19.7$ min (Figure 4G). This assignment was confirmed by subsequent LC/MS^2 analysis of the m/z 505 ion (inset of Figure 4G) and also in a D_9-POBN experiment by the EIC and LC/MS^2 of the m/z 514 ion (the D_9-POBN adduct of $^\bullet L_{18:3}(OH)_2$, Figure 4H).

Monitoring the ESR-silent redox forms of the POBN adducts greatly advanced the method's

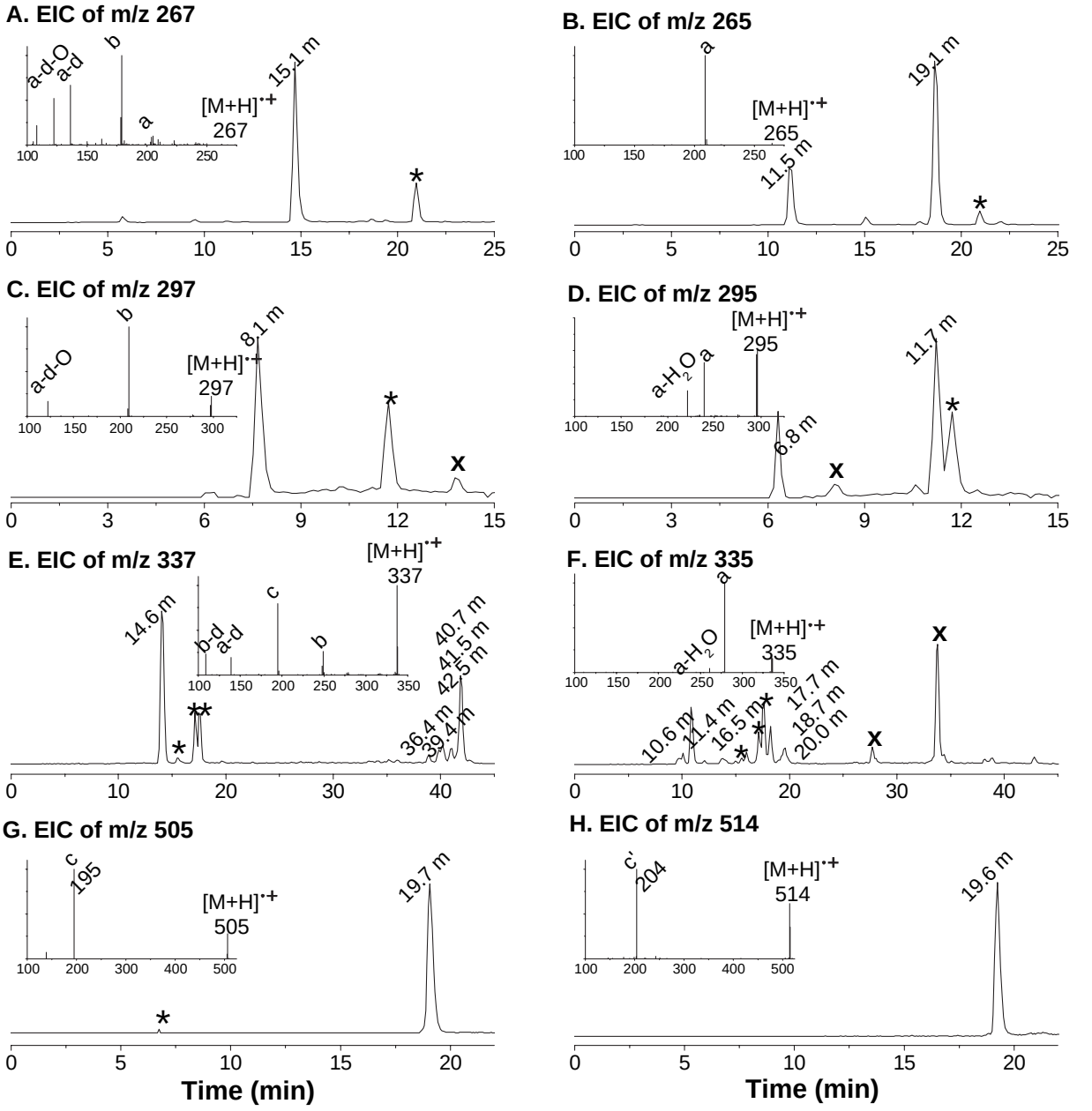

Figure 4. EICs and LC/MS^2 of ESR-silent forms of POBN adducts that were identified in Figure 3. (A) EIC and LC/MS^2 (inset) of m/z 267 ion as the reduced form of POBN/$^\bullet$C$_5$H$_{11}$; (B) EIC and LC/MS^2 (inset) of m/z 265 ion as the oxidized form of POBN/$^\bullet$C$_5$H$_{11}$; (C) EIC and LC/MS^2 (inset) of m/z 297 ion as the reduced form of POBN/$^\bullet$C$_5$H$_9$O$_2$; (D) EIC and LC/MS^2 (inset) of m/z 295 ion as oxidized form of POBN/$^\bullet$C$_5$H$_9$O$_2$; (E) EIC and LC/MS^2 (inset) of m/z 337 ion as the reduced form of POBN/$^\bullet$C$_8$H$_{13}$O$_2$; (F) EIC and LC/MS^2 (inset) of m/z 335 ion as the oxidized form of POBN/$^\bullet$C$_8$H$_{13}$O$_2$; and (G and H) EICs and LC/MS^2 (insets) of m/z 505 and m/z 514 ion (D$_9$-POBN counterpart) as oxidized form of POBN adduct of $^\bullet$L(OH)$_2$, respectively. Note that a D$_9$-POBN-related product always has retention times ~12 s shorter than its POBN counterpart under our chromatography conditions. Fragmentation patterns and *a*, *b*, *c* and *d* ions of all tested POBN adducts (*a'*, *b'*, *c'*, *d'* ions of all tested D$_9$-POBN adducts) were consistent with LC/MS^2 of POBN adducts published elsewhere [30,31] as well as those described in Scheme 1. The redox forms of the m/z 240 ion (m/z 241 and m/z 239) were not analysed because they are GLA-unrelated radicals. '×' represents POBN-unrelated EIC peak; '*' represents a portion of the ESR-active form(s) being reduced/oxidized during MS ionization.

sensitivity and reliability as the oxidized product, i.e. m/z 505 ion, had an even higher detection sensitivity (based on abundance) than the corresponding radical adduct, i.e. m/z 506 ion (Figure 4G). Based on this observation, we also tested the possibility of profiling ESR-silent forms of adducts whose ESR-active forms are not detectable in on-line ESR under our conditions. Two such types of POBN adduct are lipid alkyl radicals (L$^\bullet$) and lipid epoxyallylic radicals (OL$^\bullet$, Scheme 1), which have not always been measured with LC/ESR due to their relatively shorter lives and often lower abundance [30–32]. Although POBN/L$^\bullet$ (m/z 472) and POBN/OL$^\bullet$ (m/z 488) adducts were not detected in Figure 2, EIC peaks of m/z 473 and

m/z 489 ions that were possibly reduced forms of such adducts were profiled at $t_R \approx 35.1$ and 39.5 min (Figure 5A) and 25.9, 26.7, 28.6, 29.3 and 29.9 min (Figure 5C), respectively. Similarly, EIC peaks of m/z 471 and m/z 487 ions, possibly the oxidized forms were profiled at $t_R \approx 28.1$, 29.3, 30.3, 31.0, 31.7, 32.2, 33.3, 38.7 and 39.5 min (Figure 5E) and 29.6 min (Figure 5G), respectively. All these structural assignments were confirmed by their LC/MS^2 with both POBN (Figures 5B, D, F and H) and D_9-POBN (corresponding insets of Figures 5B, D, F and H). Again, fragmentation ions in the LC/MS^2 of those fractions failed to offer enough information to distinguish difference among the relevant isomers.

LC/MS comprehensive quantification of spin-trapped radicals

Quantification of free radical formation is critical for evaluation and interpretation of many radical mediated biological processes. Currently available ESR-based quantification protocols rely on a comparison of relative signal intensities (or signal areas) between a standard compound (internal and/or external) and the test samples. However, due to the unstable nature of free radicals, including radical adducts, all ESR-based protocols are problematic in term of becoming a reliable quantitative method. In addition, ESR and ESR-based quantitative protocols

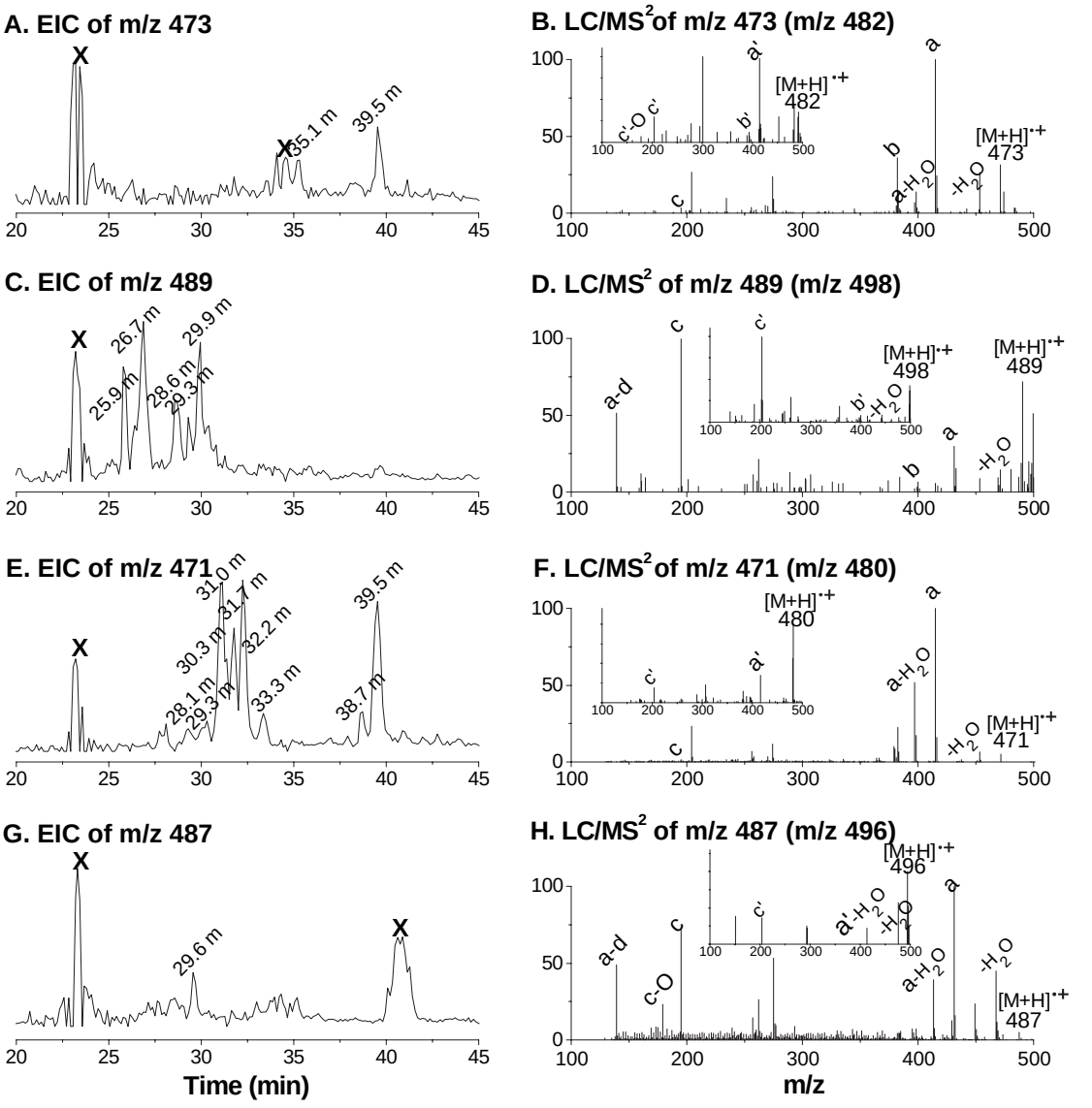

Figure 5. EICs and LC/MS^2 of ESR-silent forms of POBN/L$^\bullet$ and POBN/OL$^\bullet$. (A and B) EIC and LC/MS^2 of m/z 473 for the reduced product of POBN/L$^\bullet$, as well as LC/MS^2 of the m/z 482 ion from the D_9-POBN experiment (inset); (C and D) EIC and LC/MS^2 of m/z 489 for the reduced product of POBN/OL$^\bullet$, as well as LC/MS^2 of the m/z 498 ion from the D_9-POBN experiment (inset); (E and F) EIC and LC/MS^2 of the m/z 471 ion for the oxidized product of POBN/L$^\bullet$, as well as LC/MS^2 of the m/z 480 ion from D_9-POBN experiment (inset); and (G and H) EIC and LC/MS^2 of the m/z 487 ion for the oxidized product of POBN/OL$^\bullet$, as well as LC/MS^2 of the m/z 496 ion from the D_9-POBN experiment (inset). Note that fragmentation patterns and *a*, *b*, *c* and *d* ions of all tested products (*a'*, *b'*, *c'* and *d'* ions for the D_9-POBN experiments) were consistent with the LC/MS^2 of POBN products published elsewhere [30,31] as well as the pattern described in Scheme 1. '×' represents POBN-unrelated EIC peak.

cannot accommodate a high throughput screen due to technique limitations.

Our high throughput LC/MS analysis allowed us to simultaneously identify all three redox forms of each POBN trapped radical (see above). It has now been refined and extended to a high throughput LC/MS screen for a comprehensive quantification of each free radical's formation, with D_9-POBN used as an internal quantitative standard rather than a spin trap for radical identification. For this purpose, a small measured amount of D_9-POBN was added after the analyte was mixed with ACN to denature and precipitate LOX enzymes. When 3.8 μg/ml internal standard D_9-POBN (m/z 204 peak at $t_R \approx$ 6.8 min) was added to a solution, ~43.4 μg/ml of POBN/$^{\bullet}C_5H_{11}$ (m/z 266) was observed at $t_R \approx 21.2$ min (Figure 6A), while ~23.7 μg/ml of the reduced form (m/z 267) was seen at $t_R \approx 15.1$ min (Figure 6B) and a total of 51.9 (13.7 ± 38.2) μg/ml of two oxidized forms (m/z 265) was quantified at $t_R \approx$ 11.5 and 19.1 min (Figure 6C).

During an MS ionization, POBN adducts readily convert from one form to another. For instance, due to ongoing redox reactions inside the MS source, portions of the adduct POBN/$^{\bullet}C_5H_{11}$ (m/z 266 ion) were also detected as the reduced form (m/z 267 ion, marked with an asterisk in Figure 6B) and the oxidized form (m/z 265 ion, marked with an asterisk in Figure 6C) at $t_R \approx 21.2$ min. To comprehensively quantitate a given POBN adduct, we totalled up all of its redox forms generated both during the system reaction and inside the MS source. For example, for POBN/$^{\bullet}C_5H_{11}$, from the peak at $t_R \approx 21.2$ min, we add 5.8 μg/ml of m/z 267 (Figure 6B) and 2.4 μg/ml of m/z 265 (Figure 6C), both formed during MS ionization, to the total of the m/z 266 ion (Figure 6A) to obtain a total of 51.6 ($43.4 + 5.8 + 2.4$) μg/ml of such radical actually formed. Similarly, a total quantity of the oxidized form of POBN/$^{\bullet}C_5H_{11}$ (m/z 265, Figure 6C) could also be comprehensively accounted for by considering the redox reaction inside MS source, including m/z 266 (1.9 μg/ml + 5.7 μg/ml in Figure 6A) and m/z 267 (0.2 μg/ml + 0 μg/ml in Figure 6B) at $t_R \approx$ 11.5 and 19.1 min, to the total of 59.7 μg/ml. Comprehensive quantities of the reduced form of POBN/$^{\bullet}C_5H_{11}$ and redox forms of other POBN trapped radicals are listed in Table I. Our experiment represents the most comprehensive quantification process that we have ever been able to carry out in terms of radical detection.

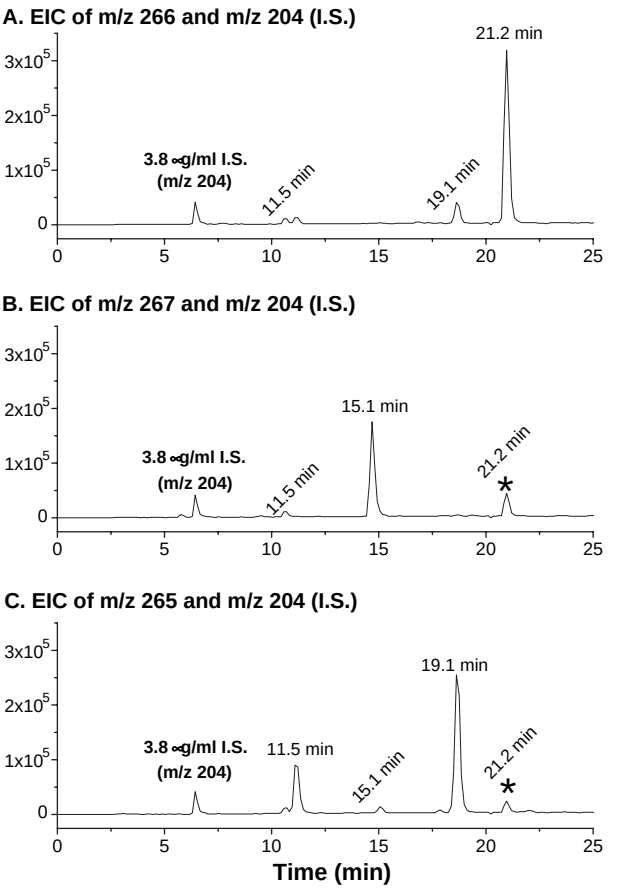

Figure 6. Comprehensive quantification of POBN/$^{\bullet}C_5H_{11}$ *via* LC/MS. (A) EIC abundance comparison of m/z 204 (3.8 μg/ml internal standard of D_9-POBN) *vs* m/z 266 (ESR-active form of POBN/$^{\bullet}C_5H_{11}$) at $t_R \approx 21.2$ min as well as at $t_R \approx 11.5$ and 19.1 min (generated from its two oxidized forms due to MS ionization); (B) EIC abundance comparison of m/z 204 *vs* m/z 267 (the reduced form of POBN/$^{\bullet}C_5H_{11}$) at $t_R \approx 15.1$ min as well as at $t_R \approx$ 11.5 and 21.2 min (generated from the oxidized form m/z 265 and the adduct form m/z 266 due to MS ionization, respectively); and (C) EIC abundance comparison between m/z 204 *vs* m/z 265 (oxidized forms of POBN/$^{\bullet}C_5H_{11}$) at $t_R \approx 11.5$ and 19.1 min, as well as at $t_R \approx 15.1$ and 21.2 min (generated from m/z 267 and m/z 266 due to MS ionization, respectively). Quantanalysis version 1.8 for Agilent 6300 Series Ion trap LC/MS was used to process the integration and calculation of peaks.

Discussion

In this work we have used the combination technique of LC/ESR and LC/MS to profile the spin adducts of carbon-centred radicals formed from soybean lipoxygenase (LOX)-catalysed GLA peroxidations in the presence of POBN. We have trapped and identified four classes of radicals, including lipid alkyl radicals ($L^{\bullet}$), lipid epoxyallylic radicals ($OL^{\bullet}$), lipid dihydroxyallylic radicals ($^{\bullet}L(OH)_2$) and a variety of carbon-centred radicals formed from β-scission of lipid alkoxyl radicals. Unlike many previous studies [30–32] in which a pH 8.5 buffer solution was used to optimize LOX activity, here we were more interested in the LOX reaction under the physiological pH of 7.4. Possibly due to this change in pH, we were unable to observe two types of GLA-derived radicals, lipid alkyl radicals ($L^{\bullet}$) and lipid epoxyallylic radicals ($OL^{\bullet}$), as ESR-active forms in our study (Figure 5 and Table I). The different pHs in reaction buffers may have caused different LOX activity.

Table I. Relative quantification of POBN adducts in all redox forms formed from LOX-catalysed GLA peroxidation.

Reaction time (min)	POBN/$^{\bullet}C_8H_{13}O_2$			POBN/$^{\bullet}C_2H_{11}$			POBN/$^{\bullet}C_2H_9O_2$			*POBN/$^{\bullet}$L		†POBN/$^{\bullet}$LO		‡POBN/$^{\bullet}$L(OH)$_2$
	Ox m/z 335	Rad m/z 336	Red m/z 337	Ox m/z 265	Rad m/z 266	Red m/z 267	Ox m/z 295	Rad m/z 296	Red m/z 297	Ox m/z 471	Red m/z 473	Ox m/z 487	Red m/z 489	Ox m/z 505
0.5	2.90±0.37	50.92±7.85	20.05±0.91	12.05±1.12	25.80±3.61	13.05±0.41	0.51±0.18	3.03±0.76	0.77±0.16	2.66±0.45	0.46±0.09	0.32±0.27	0.51±0.03	0.87±0.44
1	3.05±0.29	68.44±0.22	26.96±3.26	14.61±0.87	31.48±6.33	11.95±1.73	0.71±0.10	5.15±0.42	1.22±0.03	2.66±0.79	0.32±0.09	0.35±0.21	1.03±0.10	1.23±0.82
2	3.82±0.09	83.47±4.99	28.63±3.00	19.04±2.16	31.79±4.52	11.05±1.50	1.15±0.10	7.21±0.39	1.75±0.18	2.17±0.36	0.28±0.11	0.66±0.25	1.19±0.21	5.76±2.74
5	5.84±0.55	133.20±17.6	37.81±2.15	33.56±1.85	49.57±5.17	18.46±1.65	1.74±0.17	11.99±1.68	2.59±0.05	2.79±0.18	0.25±0.09	0.82±0.15	1.82±0.15	9.67±1.75
15	8.18±0.63	142.89±15.9	38.49±7.96	46.38±5.72	56.96±6.67	19.14±4.70	3.36±0.23	17.73±1.94	3.50±1.15	2.46±0.42	0.20±0.05	0.83±0.07	2.02±0.31	11.74±5.42
30	9.16±1.34	152.45±30.7	64.96±13.6	70.64±15.8	57.93±21.08	26.27±7.34	5.70±1.93	17.94±2.58	2.48±1.39	3.56±1.14	0.65±0.47	0.60±0.13	3.83±1.88	10.50±5.82
45	11.59±0.70	125.10±3.54	40.93±1.17	55.69±0.34	47.71±0.92	20.69±1.53	4.86±0.12	18.50±0.43	4.02±0.37	2.33±0.05	0.15±0.05	0.70±0.19	2.18±0.12	11.82±1.91
60	12.69±1.72	115.63±9.07	43.81±3.89	62.96±6.83	47.50±4.11	22.15±2.54	5.21±0.42	18.64±1.72	3.39±0.60	2.83±0.26	0.14±0.05	0.61±0.20	2.09±0.37	13.39±10.02

*,†the radical form of the POBN adduct was below the detection limit under our system conditions; ‡the reduced form of the POBN adduct was below the detection limit, while the spin adduct itself failed to produce reliable statistical data due to overlapping with the necessary overdose of POBN.

Note that 3.8 μg/ml D_9-POBN was used as an internal standard to quantify POBN trapped carbon-centred radicals as well as their redox products formed in LOX-catalysed GLA peroxidation. The ESR-active peak 2, m/z 240 for POBN/$^{\bullet}C_2H_4OH$ was not listed in the Table since it was not a GLA related radical product. Quantanalysis version 1.8 for Agilent 6300 Series Ion trap LC/MS was used to process the integration and calculation. Data are expressed as means±SD from $n \geq 3$.

The somewhat lower detection sensitivity for the above two radicals may also have resulted from the significantly lower concentration of the spin trap POBN used in this study. In fact, when pH 8.7 buffer solutions or higher concentrations of POBN ($\geq$ 60 mM) were re-established for the LOX-catalysed GLA reaction, limited amounts of both POBN/L$^{\bullet}$ and POBN/OL$^{\bullet}$ could be observed in several isomeric forms at $t_R \sim 38$–42 min and 27–30 min, respectively, in LC/ESR as well as LC/MS (data not shown).

If the chromatographic fraction of a radical adduct and/or its redox forms is low, it normally results in a poor quality LC/MS^2 spectrum, whose fragmentation pattern sometimes fails to contain enough information to confirm the proposed structure. In this case, LC/MS^2 coupled with a combination of POBN and D_9-POBN spin trapping experiments offers a unique and powerful identification strategy for such structural confirmation [36,37]. For any given radical that was trapped, the observation of identical LC/MS^2 fragmentation patterns for both a POBN and a D_9-POBN adduct confirms the structure even with poor quality MS spectra. For example, identical fragments caused by losing a radical ($^{\bullet}$R) from POBN and D_9-POBN adducts (9-Da difference between their protonated molecules) leads to the observation of pair(s) of fragment ions differing by 9 Da, such as m/z 195 (*c* ion) and m/z 204 ions (*c'* ion) as POBN and D_9-POBN, respectively (Figures 3E and F, 4G and H and 5B, D, F and H). Other unique pairs always observed include those involving the loss of the *tert*-butyl groups of POBN, *i.e. a* and *b* vs *a'* and *b'* ions (where hydrogen was replaced by deuterium in D_9-POBN). In addition, each counterpart of given D_9-POBN-trapped radicals or related derivatives had a retention time $\sim$12 s shorter than that from the corresponding POBN experiment under our separation conditions. All of these features make this analysis extremely valuable for structural identification of all redox forms of POBN adducts.

Considering the common reducing environment in cellular and *in vivo* systems, the ability to identify two ESR-silent forms in addition to the ESR-active form of a POBN adduct may offer a great improvement in sensitivity and reliability in terms of radical detection in many biological systems. For the first time, we were able to take into account the redox reactions of a spin adduct as well as the remaining radicals formed during lipid peroxidation to obtain the overall original free radical production. In general, fragmentation patterns of reduced products in LC/MS^2 are much like those of the corresponding ESR-active products showing the major fragmentation ions, *a*, *b*, *c* and *d* (Scheme 1) [30–32]. However, the oxidized product of a POBN adduct has some distinct features in MS analysis. The fragmentation ion of -87 Da (ion *b*) does not exist in oxidized products since the double

bond (C = N) formed in nitrone adducts eliminates such fragmentation (Scheme 1). In addition, more isomers of the oxidized form were sometimes identified than were present in the original adduct or the relevant reduced isomers, most likely due to the formation of geometric isomers (E and Z) from the newly formed double bond.

The reliability of traditional ESR quantification protocols, whether internal or external, has always been questioned since a structurally different standard compound must be used. Different procedures (due to the structural difference) must be used to quantify electron density in an internal standard and the test compounds, which generally results in unreliable radical quantification. An external ESR standard may have a limited advantage on this issue since it can be selected for a structure similar to the test products. In addition, when radical measurement must be followed with sample handling, *e.g.* lipid extraction procedure, chromatographic separation or even simple dilution/condensation with an organic solvent for enzyme precipitation, additional problems are introduced; it is then impossible to accomplish radical quantification with any type of ESR standards or protocols appropriately.

Selecting an appropriate standard for our LC/MS was critical for reliable quantification. Based on our observations, all redox forms of the radical adduct most likely share a common moiety (the nitrone attached to pyridyl ring) with POBN as the preferred position for protonation during MS ionization (Scheme 1). This factor suggested D_9-POBN as a suitable internal standard. Due to the ease of redox reactions in any adduct, reliable quantification of radical formation had to take into account all its redox forms generated not only during the system reaction, but also during MS ionization. Although questions of quantitative reliability may still be raised due to different analyte's responses towards MS ionization with the same or different mobile phase ratios, there is no doubt that our protocol is presently the most comprehensive for quantitation of radical formation.

Because of the possible different trapping rates and different extent of ionization in MS for a variety of free radicals and adducts, the data of Table I represents relative quantities of POBN adducts. However, the result, e.g. three major β-scission products, could be used to estimate relative formation of products of LOX-catalysed GLA peroxidation on different carbons since their corresponding precursor metabolites, LOOHs (9-LOOH, 13-LOOH and 6-LOOH), showed the same or nearly the same ratios as those of the quantities of adducts in Table I. We were able to monitor those LOOHs using normal phase LC/MS with appropriate standards (data not shown). For the GLA-derived radicals listed in Table I, three major β-scission products were observed in the order $^{\bullet}C_8H_{13}O_2 > {}^{\bullet}C_5H_{11} > {}^{\bullet}C_5H_9O_2$. This result indicated that oxygen preferentially reacts with the 9-, 13- and 6-carbons in GLA under our conditions (Scheme 1). Overall free radical profiles did not show significant changes during a 1 h reaction according to their LC/ESR/MS analysis (Table I). This result was confirmed by an oxygen consumption experiment (data not shown) in which most of the radical reaction appears to occur within the first 45 s, during which time $>90\%$ of the oxygen was consumed in the reaction solution. At 30 min, the overall radical formation reached a plateau and started to decrease afterward, most likely because the decomposition reactions of the spin adducts began to dominate compared to the spin trapping reaction. However, the methods in this study certainly provide a means to analyse radical formation in cellular or *in vivo* lipid peroxidation currently ongoing in our laboratory, since a steady state of $[O_2]_{ss}$ is always available.

Acknowledgements

This work was supported by NIEHS Grant ES-012978.

***Declaration of interest*:** The authors report no conflicts of interest. The authors alone are responsible for the content and writing of the paper.

References

[1] Fan YY, Chapkin RS. Importance of dietary g-linolenic acid in human health and nutrition. J Nutr 1998;128:1411–1414.
[2] Harbige LS. Fatty acids, the immune response, and autoimmunity: a question of n-6 essentiality and the balance between n-6 and n-3. Lipids 2003;38:323–341.
[3] Calder PC, Zurier RB. Polyunsaturated fatty acids and rheumatoid arthritis. Curr Opin Clin Nutr Metab Care 2001;4:115–121.
[4] Darlington LG, Ramsey NW. Review of dietary therapy for rheumatoid arthritis. Compr Ther 1994;20:490–494.
[5] Horrobin DF. Essential fatty acid metabolism and its modification in atopic eczema. Am J Clin Nutr 2000;71:367S–372S.
[6] Pham H, Vang K, Ziboh VA. Dietary γ-linolenate attenuates tumor growth in a rodent model of prostatic adenocarcinoma via suppression of elevated generation of PGE2 and 5S-HETE. Prostaglandins Leukot Essent Fatty Acids 2006;74:271–282.
[7] Menendez JA, del Mar Barbacid M, Montero S, Sevilla E, Escrich E, Solanas M, Cortes-Funes H, Colomer R. Effects of γ-linolenic acid and oleic acid on paclitaxel cytotoxicity in human breast cancer cells. Eur J Cancer 2001;37:402–413.
[8] Cantrill RC, Ells G, Chisholm K, Horrobin DF. Concentration-dependent effect of iron on γ-linolenic acid toxicity in ZR-75-1 human breast tumor cells in culture. Cancer Lett 1993;72:99–102.
[9] Perabo FG, Muller SC. New agents in intravesical chemotherapy of superficial bladder cancer. Scand J Urol Nephrol 2005;39:108–116.

[10] Harris NM, Crook TJ, Dyer JP, Solomon LZ, Bass P, Cooper AJ, Birch BR. Intravesical meglumine γ-linolenic acid in superficial bladder cancer: an efficacy study. Eur Urol 2002;42:39–42.
[11] Ravichandran D, Cooper AC, Johnson CD, Karran SJ. Growth inhibitory effect of lithium salt of gamma linolenic acid on human pancreatic cancer cells *in vitro*. Gastroenterology 1995;108:A528.
[12] Das UN. From bench to the clinic: γ-linolenic acid therapy of human gliomas. Prostaglandins Leukot Essent Fatty Acids 2004;70:539–552.
[13] Bakshi A, Mukherjee D, Bakshi A, Banerji AK, Das UN. γ-linolenic acid therapy of human gliomas. Nutrition 2003;19: 305–309.
[14] Vang K, Ziboh VA. 15-lipoxygenase metabolites of γ-linolenic acid/eicosapentaenoic acid suppress growth and arachidonic acid metabolism in human prostatic adenocarcinoma cells: possible implications of dietary fatty acids. Prostaglandins Leukot Essent Fatty Acids 2005;72:363–372.
[15] Watkins G, Martin TA, Bryce R, Mansel RE, Jiang WG. γ-Linolenic acid regulates the expression and secretion of SPARC in human cancer cells. Prostaglandins Leukot Essent Fatty Acids 2005;72:273–278.
[16] Vartak S, McCaw R, Davis CS, Robbins ME, Spector AA. Gamma-linolenic acid (GLA) is cytotoxic to 36B10 malignant rat astrocytoma cells but not to 'normal' rat astrocytes. Br J Cancer 1998;77:1612–1620.
[17] Das UN. Essential fatty acids, lipid peroxidation and apoptosis. Prostaglandins Leukot Essent Fatty Acids 1999;61:157–163.
[18] Ramanathan R, Das NP, Tan CH. Effects of γ-linolenic acid, flavonoids, and vitamins on cytotoxicity and lipid peroxidation. Free Radic Biol Med 1994;16:43–48.
[19] Sagar PS, Das UN, Koratkar R, Ramesh G, Padma M, Kumar GS. Cytotoxic action of cis-unsaturated fatty acids on human cervical carcinoma (HeLa) cells: relationship to free radicals and lipid peroxidation and its modulation by calmodulin antagonists. Cancer Lett 1992;63:189–198.
[20] Das UN. Tumoricidal action of cis-unsaturated fatty acids and their relationship to free radicals and lipid peroxidation. Cancer Lett 1991;56:235–243.
[21] Girotti AW. Mechanisms of lipid peroxidation. Free Radic Biol Med 1985;1:87–95.
[22] Gardner HW. Oxygen radical chemistry of polyunsaturated fatty acids. Free Radic Biol Med 1989;7:65–86.
[23] Janzen EG, Blackburn BJ. Detection of and identification of short-lived free radicals by an electron spin resonance trapping technique. J Am Chem Soc 1968;90:5909–5910.
[24] Janzen EG. Spin trapping. Acc Chem Res 1971;4:31–40.
[25] Kadiiska MB, Mason RP, Dreher KL, Costa DL, Ghio AJ. *In vivo* evidence of free radical formation in the rat lung after exposure to an emission source air pollution particle. Chem Res Toxicol 1997;10:1104–1108.
[26] Kadiiska MB, Morrow JD, Awad JA, Roberts LJ, Mason RP. Identification of free radical formation and F_2-isoprostanes *in vivo* by acute Cr(VI) poisoning. Chem Res Toxicol 1998;11:1516–1520.
[27] Qian SY, Buettner GR. Iron and dioxygen chemistry is an important route to initiation of biological free radical oxidations: an electron paramagnetic resonance spin trapping study. Free Radic Biol Med 1999;26:1447–1456.
[28] Qian SY, Wang HP, Schafer FQ, Buettner GR. EPR detection of lipid-derived free radicals from PUFA, LDL, and cell oxidations. Free Radic Biol Med 2000;29:568–579.
[29] Buettner GR. Spin trapping: EPR parameters of spin adducts. Free Radic Biol Med 1987;3:259–303.
[30] Qian SY, Guo Q, Mason RP. Identification of spin trapped carbon-centered radicals in soybean lipoxygenase-dependent peroxidations of ω-3 polyunsaturated fatty acids by LC/ESR, LC/MS, and tandem MS. Free Radic Biol Med 2003;35:33–44.
[31] Qian SY, Yue GH, Tomer KB, Mason RP. Identification of all classes of spin-trapped carbon-centered radicals in soybean lipoxygenase-dependent lipid peroxidations of ω-6 polyunsaturated fatty acids via LC/ESR, LC/MS, and tandem MS. Free Radic Biol Med 2003;34:1017–1028.
[32] Qian SY, Tomer KB, Yue GH, Guo Q, Kadiiska MB, Mason RP. Characterization of the initial carbon-centered pentadienyl radical and subsequent radicals in lipid peroxidation: identification via on-line high performance liquid chromatography/electron spin resonance and mass spectrometry. Free Radic Biol Med 2002;33:998–1009.
[33] Buettner GR. In the absence of catalytic metals ascorbate does not autooxidize at pH7: ascorbate as a test for catalytic metals. J Biochem Biophys Meth 1988;16:27–40.
[34] Albro PW, Knecht KT, Schroeder JL, Corbett JT, Marbury D, Collins BJ, Charles J. Isolation and characterization of the initial radical adduct formed from linoleic acid and α-(4-pyridyl 1-oxide)-N-tert-butylnitrone in the presence of soybean lipoxygenase. Chem Biol Interact 1992;82:73–89.
[35] Ortiz de Montellano PR, Augusto O, Viola F, Kunze KL. Carbon radicals in the metabolism of alkyl hydrazines. J Biol Chem Biol Interact 1983;258:8623–8629.
[36] Qian SY, Chen YR, Deterding LJ, Fann YC, Chignell CF, Tomer KB, Mason RP. Identification of protein-derived tyrosyl radical in the reaction of cytochrome c and hydrogen peroxide: characterization by ESR spin-trapping, HPLC and MS. Biochem J 2002;363:281–288.
[37] Qian SY, Kadiiska MB, Guo Q, Mason RP. A novel protocol to identify and quantify all spin trapped free radicalsfrom in vitro/in vivo interaction of $HO^{\bullet}$ and DMSO: LC/ESR, LC/MS, and dual spin trapping combinations. Free Radic Biol Med 2005;38:125–135.
[38] Wilcox AL, Marnett LJ. Polyunsaturated fatty acid alkoxyl radicals exist as carbon-centered epoxyallylic radicals: a key step in hydroperoxide amplified lipid peroxidation. Chem Res Toxicol 1993;6:413–416.